RADIATION GAS DYNAMIC PROCESSES IN AN EXPLOSION CAUSED BY HIGH-VELOCITY IMPACT OF A COSMIC BODY IN MARS' ATMOSPHERE

A. V. Dobkin, T. V. Loseva, I. V. Nemchinov, I. A. Trubetskaya, and V. V. Shuvalov

UDC 533.6.011:51

Impacts of rapidly moving cosmic bodies (meteoroids, asteroids, and comets) on a planet's surface initiate explosive processes in the solid material of the planet and in its atmosphere as well. Evolution of the processes is determined not only by the body's parameters (velocity, mass, composition) and by features of the planet's surface layers, but also by the parameters of the atmosphere (mainly its density). The density of Mars' atmosphere is much lower than that of the Earth's atmosphere (100 times), and all the more of Venus (5000 times), which determines the specific features of evolution of explosions caused by the impact of cosmic bodies on the planet's surface.

During passage through the atmosphere, cosmic bodies lose their velocity and mass. The deceleration and ablation are found to be insignificant for large-sized bodies, namely, for $R_0 >> R_H = (\rho_\alpha/\rho_0)H$ (ρ_α is the atmosphere density near the planet's surface, ρ_0 is the density of the body, H is the characteristic altitude of the atmosphere [1-3]).

For stone and ice bodies moving through Mars' atmosphere, R_H is equal to 3 and 10 cm. For the Earth's atmosphere these values are two orders of magnitude greater, that is, 3 and 10 m.

Aerodynamic forces may destroy the cosmic body during its passage through the atmosphere. It may intensity the deceleration of originated swarms of fragments and even result in a blast above the planet's surface [3-5]. In Mars' atmosphere, aerodynamic loadings are considerably lower than those observed in the passage of a body through the Earth's atmosphere, all the more through Venus' atmosphere. Thus, the maximum pressure p_m at the front dull nose of a body moving through the atmosphere near Mars' surface at a velocity of 30-50 km/sec is as low as 100-300 bar. However, if the body is not a monolith, even these moderate pressures may cause the body to be broken into fragments, as is demonstrated by data on meteor destruction in the Earth's atmosphere [6-9].

The compressible fluid approximation is often used to describe the deformation of a destroyed body [1, 9]. Estimates [1] show that the velocity of the lateral material flow is of the order of $\sqrt{(\rho_\alpha/\rho_0)}V$ (V is the body's velocity), so deformation and destruction are negligible for large bodies ($R_0 > R_c = (\rho_\alpha/\rho_0)^{1/2}$ H) passing through a layer of thickness H, the characteristic altitude of the atmosphere. For Mars the critical size R_c is 17 and 30 m for a body of stone and ice, and for the Earth it is 170 and 300 m. However, even though a body is destroyed, its fragments do not spray too far – at a range close to R_c. When the energy of the body is high enough, blast waves, generated by each impact in both the planet's material and its atmosphere, merge, and shortly after the impact, the process can be treated as a unit exposition with total energy.

High-velocity impact on the planet's surface results in fusion and evaporation of both the body and the planet's surface material [10, 11]. Rough estimate of the μ ratio of the evaporated mass M_v to the initial body's mass M_0 can be carried out using the solution of the short concentrated impact problem [12]. The results of calculations [10] concerning iron meteorite impacts on silicate rocks are in agreement with these estimates and provide μ values close to 100. The μ values for an ice body are one order of magnitude less.

A shock wave in the atmosphere is generated by an expanding hot "torch" of vapor, condensate droplets, and fused material ("explosion products") [10, 11].

The characteristic distance R_T for the deceleration of the explosion products and the energy transfer from the torch to the atmosphere can be estimate by

$$R_T = R_0\mu^{1/3}(\rho_\alpha/\rho_0)^{-1/3}.$$

Moscow. Translated from Prikladnaya Mekhanika i Tekhnicheskaya Fizika, No. 6, pp. 35-45, November-December, 1993. Original article submitted October 12, 1992.

0021-8944/93/3406-0775$12.50

In Mars' atmosphere, when $\mu = 10$, we get $R_T = 0.1$-3 km for an ice body of size $R_0 = 1$-30 m, so deceleration is significant at distances greater than R_c, the spray distance for the fragments of the destroyed body. Thus, even in the case of a destroyed body, the atmospheric phenomenon may be considered as the deceleration of an integrated jet of the explosion products. On the other hand, the obtained distance R_T is far less than the characteristic altitude H of the atmosphere. Due to the estimates mentioned above, $R_T = 10$ km at $R_0 \approx 100$ m, so $R_T \approx H$, and atmosphere nonhomogeneity should be reckoned with even at the deceleration stage, but a moving body has time to transfer its kinetic energy to the atmospheric gas. For very large bodies with $R_T >> H$ the atmosphere is not significant at all, and a part of its mass close to $(2\pi/3)\rho_\alpha{}^0H^3$ is just ejected with the explosion products at velocities close to the impact velocity V. Hereafter, we shall consider only the impacts of not-too-large and not-too-small bodies (for ice bodies $R_0 = 1$-100 m), when there is insignificant or no fragmentation, and the energy of a decelerating body transfers to the atmosphere.

Investigations of the evolution of explosions caused by impacts of cosmic bodies of size $R_0 = 1$-100 km are motivated by the following. Essential to the evolution of the planet's atmosphere, there is a problem of ejection of the material of both the cosmic body and the planet to the upper atmosphere and its "pollution" after the impact.

Another recent broadly discussed problem is the danger from asteroids. The probability of large (0.3-1 km and more) asteroid impacts is determined via astronomic observations by optical and radiolocative means. However, the impacts of such bodies are rather rare, whereas the impacts of bodies of 10-100 m in size may lead to a catastrophe. One method of determining the distribution function of these bodies in the solar system is to observe body impacts.

For small bodies, not only $R_T << H$, but also the limiting sizes of the heated zone, expand after the explosion, $R_\alpha << H$. The size of the resulting fireball [10, 13] can be estimated by the relationship

$$R_\alpha = R_0 M_\alpha{}^{2/3}[\gamma(\gamma - 1)\rho_0/\rho_\alpha]^{1/3},$$

where $M_\alpha = V/C_\alpha$ is the Mach number, C_α is the speed of sound in air, and γ is the adiabatic index for heated air. For V = 50 km/sec, $\gamma = 1.24$, and $R_0 = 1$-10 m we obtain $R_\alpha = 0.7$-7 km, that is, $R_\alpha < H$. Late in the explosion (when the radius of the shock wave front $R_S > R_T$), its development closely resembles the development of spot mass-free explosion. Thermal emission from hot plasma, consisting of explosive products and heated atmospheric gas behind the shock wave front, may be of importance in the development of the explosion. It is known that loss of energy reaches 30% for strong explosions near the Earth's surface [12].

A simple way to estimate the role of thermal emission in explosions near Mars is to use the results of calculations for air explosions near the Earth's surface at altitudes where the air density corresponds to the density of the atmosphere near Mars' surface. Calculations [14-16] show that when the air density is about 0.01 of normal, the portion of the incandescent energy increases and reaches 60-70% and more, and the incandescence time decreases. From these estimates, one would expect the role of thermal emission in explosions near Mars' surface to be important. Let us consider this factor in greater detail.

We note first that a blackbody's thermal flux $\sigma T_S{}^4$ (σ is the Stefan–Boltzmann constant, T_S is the gas temperature behind the shock wave front) is greater than the hydrodynamic flux of energy $(1/2)\rho_\alpha D^3$ (D is the shock wave velocity) when $T_S > 2.7$ eV or D > 21 km/sec. Thus, in Mars' atmosphere, the critical velocities are markedly lower than those in air of normal density (about 27 eV and 90 km/sec [12]). Shock wave emission at high temperature behind its front is mainly in the vacuum-ultraviolet part of the spectrum and is absorbed near the front. It forms the so-called heating layer. According to theory [12], the maximum temperature ahead of the front T_- is defined by the parameter $\eta = \sigma T_S{}^4/((1/2)\rho_\alpha D^3)$ for subcritical waves. For supercritical waves the temperature T_- is close to T_S, and the heating layer grows in width because of intense radiant transfer of the type of radiant thermal conductivity. Only a small portion of the radiation from the forward, relatively cool edge of a thermal wave, moving in front of the hydrodynamic jump, is emitted at considerable distance from the front. Radiation becomes intense only after the wave becomes subcritical (the so-called first maximum of radiation).

The nature of the emission essentially depends on the optical thickness τ of the plasma behind the shock wave front. When $\tau >> 1$, the shock wave glows, and the distribution of temperature and density insidethefireballhasnoinfluenceon the energy losses. In this case the radiation flux is totally defined by the velocity D, the radius r_S, and the shape of the shock wave surface. The dependence of the blackness coefficient $\chi = \int_0^\infty B_\varepsilon (1 - e)^{-Xk_\varepsilon} d\varepsilon / \int_0^\infty B_\varepsilon d\varepsilon$ on the temperature T in a uniformly heated layer of thickness X = 10 and 100 mispresented in Fig. 1 a and Fig. 1b, respectively (the density values are indicated near each curve). When $\rho \sim 3\cdot10^{-2}$ kg/m^3, such thickness has a shock-compressed layer with $r_S = 100$ m and $r_S \sim 1$ km.

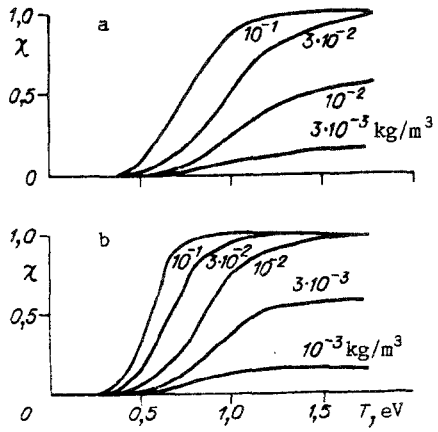

Fig. 1

Here B_ε is Planck's function, and k_ε is the absorption coefficient for photons of energy ε. We notice that the shock-compressed layer is not optically transparent when $T_S > 0.7$ eV.

Thus, to find the incandescent energy at this stage, it is sufficient to define the dependence of q_∞, the density of the radiation flux emitted at considerable distances, on the wave velocity D.

A rough estimate of gas for q_∞ for a subcritical shock wave is made under the assumption that the spectrum is defined as Planckian, corresponding to the shock wave front temperature, but is cut off at some boundary of atmosphere transparency, so that $q_\infty = \sigma T_S^4 \xi(\varepsilon_*/T_S)$ (ξ is the emission portion for quanta with energies ε, which are less than the boundary energy ε_*). On the one hand, this assumption must be verified, and on the other, the transparency boundary ε_* must be defined. In this connection, the structure and brightness of a strong shock wave in Mars' atmosphere were calculated by a procedure similar to that used in calculating them in air [14, 17].

A plain, symmetric, nonsteady spectral radiation-gas dynamic problem is investigated taking into detailed consideration the spectrum and angular direction of the emission. The thermodynamic and optical properties used here are calculated for the following mixture: 97% CO_2 and 3% N_2. Spectral absorption coefficients for comparable low temperatures ($T \leq 2$ eV) are calculated by the method [18]. Except for the atomic components C, O, N and their ions, the molecular absorption of the components CO_2, CO, C_2, C_3, O_2, CN, N_2, NO, N_2^+, O_2^+ is taken into account. Detailed tables of the spectral absorption coefficients, calculated by the method of [19, 20], are used for high temperatures.

Calculations are carried out for several hundred spectral intervals along 25 rays, which are directed at different angles from the wave propagation direction. The structure of the shock wave front is presented in Fig. 2 for gas velocities $U_S = 12.5$ km/sec and 17 km/sec (lines 1 and 2) behind the front. It closely corresponds to the qualitative pattern described in [12]. Far from the front the temperature is about 0.3 eV lower than T_S. This is connected with the fact that a portion of the emission ($q_\infty \simeq 0.57$ MW/cm^2) escapes far away. The thickness of the temperature peak at which radiation flux escapes from the front is about 1 cm, which is much lower than the thicknesses of the shock-compressed layer in the problem in question. The shock wave is subcritical, $\varepsilon_* \simeq 5.2$ eV.

Figure 3a, b show the brightness temperatures T_ε and emission spectrum $\varphi_\varepsilon = I_\varepsilon / \int I_\varepsilon d\varepsilon$ (I_ε is the emission intensity) for a velocity $U_S = 17$ km/sec at the instant $t = 76$ μsec when the wave travels 136 cm. The brightness temperature and spectral composition of the emission escaping far away at that instant of time are shown in Fig. 3c, d. A series of calculations and agreed estimates enable us to obtain the function $q_\infty(D)$.

Table 1 presents the dependence of T_S, ρ_S/ρ_0, q_α on the shock wave velocity D (the temperature, compression, and hydrodynamic flux) obtained from the shock adiabat for the corresponding shock wave velocity where q_∞ is emission escaping far away.

Let us consider the results of calculations of shock wave parameters of a spherical-symmetric explosion, caused by the impact of an ice body 10 m in radius R_0 and 4 ktons in mass M_0, moving at a velocity of 50 km/sec. The body's kinetic energy is 1.2 Mton. The bulk of the energy of explosion products of mass $10\,M_0 = 49$ kton, is transferred to Mars' atmosphere rather rapidly. Figure 4 presents the dependences of the radius of the shock wave front R_S, the front temperature T_S, and the parameter η on time t. We notice that the shock wave is close to critical for a rather long period, and the role of emission is significant. Estimates based on Table 1 allow us to determine the incandescent energy for the first 0.05 sec to be 50 kton or about 5% of the initial energy. From this time on, the two-dimensional nature of the nascent gas dynamic flow is essential. At this stage we solve the two-dimensional equations of gas dynamics with regard to gravitation, actual temperature, distribution and density in Mars' atmosphere [22].

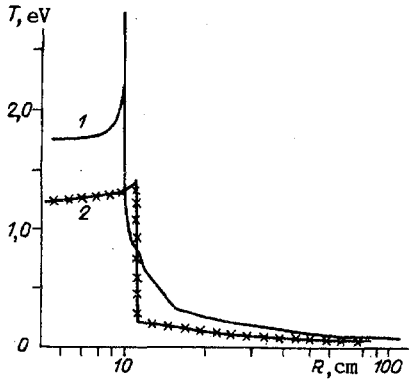

Fig. 2

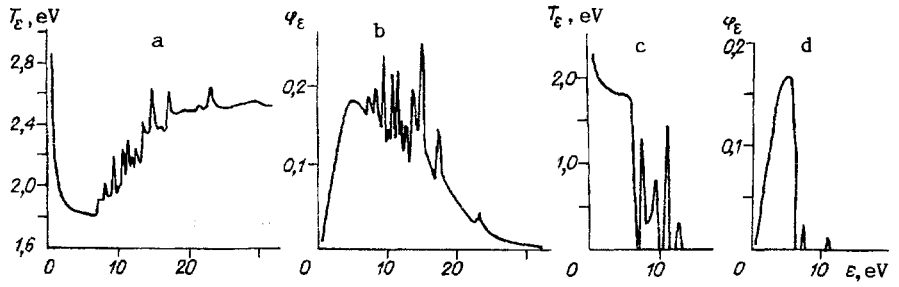

Fig. 3

As mentioned above, the portion of the incandescent energy is about 5% at the early stage ($t < 0.04$ sec.). However, emission plays an important role in energy redistribution in the inner region of a flow. Since optical thicknesses are great at high initial temperatures and densities, approximation of the radiant heat conductivity is useful for the description of radiant transfer within a luminous region, and it is used in calculations for the intermediate stage of explosion. Three reasons for the disruption of the spherical symmetry of the blast wave are considered: the initial inhomogeneity of the dense atmosphere, the onset of a "warm layer" near the planet's surface, and the trace of the moving meteoroid. The trace is considered in a simplified manner. The emitting energy is assumed to be equal to $V^2/2$ in a vertical cylinder of radius R_0, with the lower boundary of the energy-emitting zone moving down at velocity V to the point of impact and explosion. Note that the trace parameters of the meteor, including its temperature and density, are, to a large degree, specified not only by gas dynamic but also by radiation processes.

Based on the described calculations of radiation intensity from the shock wave front, we determine the fluxes of radiation energy falling upon the planet's surface at different distances R from the point of impact of the cosmic body. Figure 5 presents the density q of the fluxes and the delivered energy $W = \int_0^t q dt$ for R = 1 km and 2 km as functions of t. The maximum flux is about 10 kW/cm^2 for R = 1 km (curve 1) at t = 0.05-0.6 sec, and 0.8 kW/cm^2 for R = 2 km (curve 2). In this case the delivered energy is about 400 and 40 J/cm^2, respectively, at the same instants. Straightforward calculations and experiments on millisecond pulses of laser radiation [23] show that the values of q and W are sufficient to heat the surface of opaque materials with low heat conductivity up to the phase transition temperature, when evaporation takes effect. The amount of energy per unit area is sufficient to evaporate a surface layer 10^{-3} cm in thickness at distances close to 2 km (at the typical enthalpy of phase transition Q = 10-20 kJ/g). It is less than the thickness of the heated layer (10^{-2} cm) resulting from surface heating for 0.05 sec at the typical temperature conductivity of rocks $5 \cdot 10^{-3}$ cm^2/sec. But we should keep in mind that the planet's surface is covered with dust and sand, so its heat conductivity is small. Thus, with some confidence, the thin surface layer would be expected to evaporate at the indicated distances.

In a low density atmosphere the evaporated layer rapidly expands and forms a heated layer of large thickness. The expansion can be described under the assumption that the vapor pressure is close to the atmospheric p_α, and the vapor temperature is equal to the phase transition temperature. In this case the velocity v of the vapor boundary is determined by

$$v = \frac{m_t}{\rho_v} = \frac{qR_A T_v(\gamma - 1)}{Q p_\alpha \gamma}.$$

Here m_t is the mass consumption rate per unit area per unit time, ρ_v is the vapor density, q is the radiation flux falling on the surface, R_A is the gas constant, and γ is the adiabat. Assuming that $\gamma = 1.4$, the ratio $R_A T_v/Q$ is equal to its conventional

TABLE 1

D, km/sec	T_s, eV	ρ_s/ρ_0	q_α	q_∞	$\eta = q_\infty/q_\alpha$, %
			MW/cm^2		
7	0,64	1,67	0,17	0,014	8,2
10	0,98	1,61	0,50	0,068	13,6
12,5	1,40	1,42	0,98	0,20	20,4
15	1,72	1,36	1,69	0,36	21,2
17	2,10	1,26	2,45	0,57	23,8
20	2,89	1,12	4,00	1,29	32,2

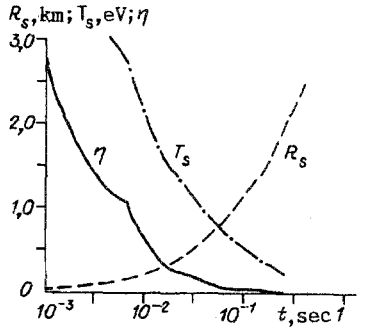

Fig. 4

value 1/6, and that the pressure p_v = 6 Mbar, we obtained v = 0.4 km/sec for q = 0.7 kW/cm^2. This velocity value is much lower than the speed of sound c_v in vapor (at T = T_v), while the expansion at such velocities results in an atmosphere shock wave, starting from the surface, with pressure slightly more than that of atmosphere, so that the pressure-equalization approximation is justified. In a time of 0.05 sec the thickness approaches 20 m for a vapor layer with such velocities. In the calculations we assume that near the surface, up to R = 2 km, a hot layer is generated at atmospheric pressure with density 10 times less than that of the atmosphere. Note that due to theoretical and experimental investigations on the warm layer effect [24], a precise value of the layer thickness is not important.

We present now numerical results for the two-dimensional radiation-gas dynamic problem with regard to the nonhomogeneity of the atmosphere, the warm layer effect, and the trace for a ice body of size R_0 = 10 m and velocity V = 50 km/sec.

Figure 6 shows isolines of the relative density ρ/ρ_h (ρ_h is the density of atmospheric gas at height h) in the lower part of a fireball at t = 0.1 sec. We observe a precursor appearing along the planet's surface due to the warm layer. In the precursor the atmospheric gas movement is vortex-like, and the precursor sizes grow with time. Movement of this type leads to a large body of sand and dust being swept away from the planet's surface. Markers, located initially inside the warm layer, are shown in Fig. 7 at t = 0.1 sec. Later the warm layer disappears, but the vortex keeps on moving some distance, initiating the pulsed local dust storm. As the body's size and explosion energy grow, the role of the warm layer increases in importance, because the portion of incandescence is conserved at the initial stage, and a definite amount of specific energy E, initiating evaporation, is achieved at a distance $R \sim \varepsilon^{1/2} \sim R_0^{3/2}$, whereas the fireball size increases in proportion to R_0.

As the precursor disappears, the shock wave is almost spherical-symmetric for about 16 sec, except for its upper part with a trace in it. The precursor appears along the trace too. Because the density in the trace is about 10 times less than that in the surrounding gas, the shock wave moves faster along the trace, and a jet appears, moving up and away from the surface. This is confirmed in Figs. 8 and 9, which show the isobars (the pressure lines p/p_α^0, p_α^0 is the pressure near the Mars' surface) and isotherms (the temperature T is measured in eV) at t = 1.1 sec. At the instant t = 0.1 and 1 sec the temperature of the shock wave front falls down to 0.7 and 0.45 eV. At these temperatures the shock wave becomes transparent and the size of the emitting fireball is smaller than the size of the high-pressure region behind the shock wave front.

The spectra of thermal radiation, emitted by the luminous region ($\varphi_\varepsilon = I_\varepsilon/I$, where I_ε is the radiation intensity at the fronts with energy ε and $I = \int_0^\infty I_\varepsilon d\varepsilon$), are obtained by solving the transfer equation for distinct ε and distinct rays intersecting the disturbed region. Figure 10 shows the spectra at t = 0.2, 0.4, 0.7, and 1.1 sec for the ray interesting the explosion center

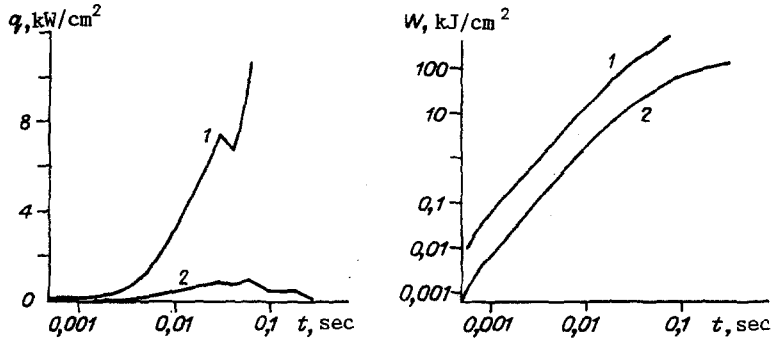

Fig. 5

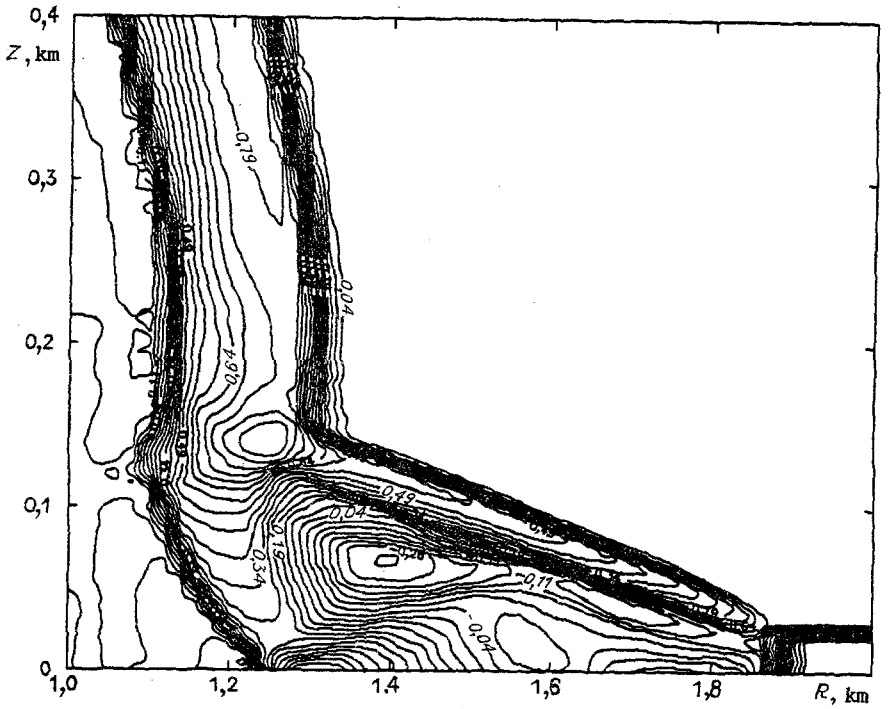

Fig. 6

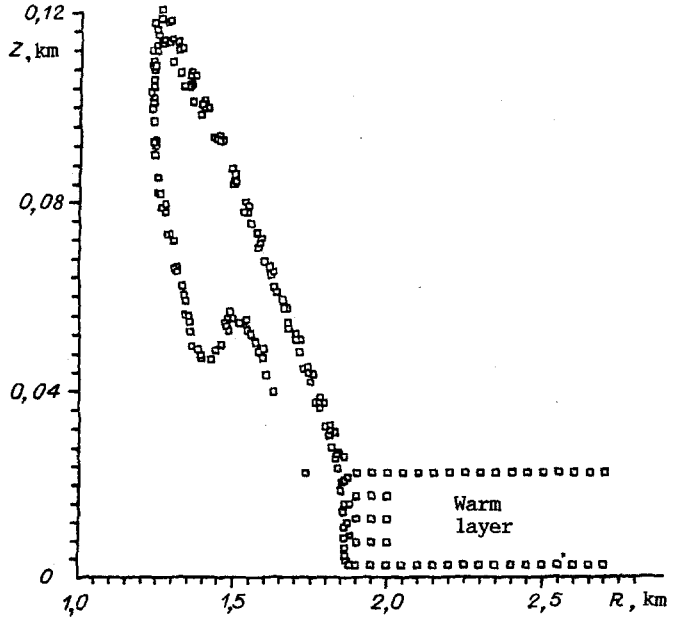

Fig. 7

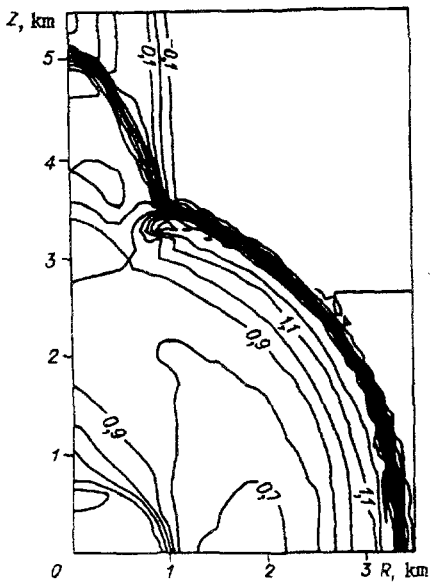

Fig. 8

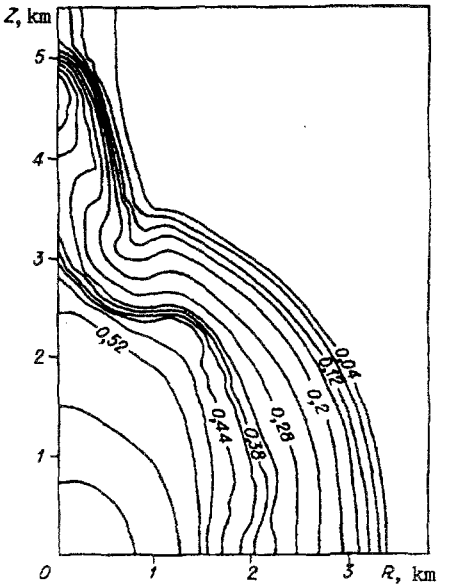

Fig. 9

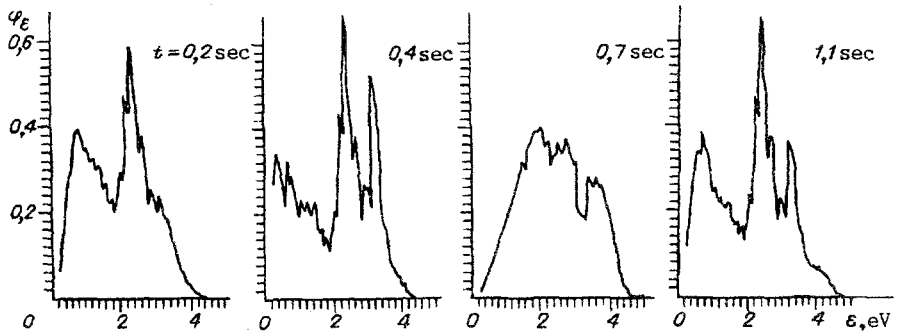

Fig. 10

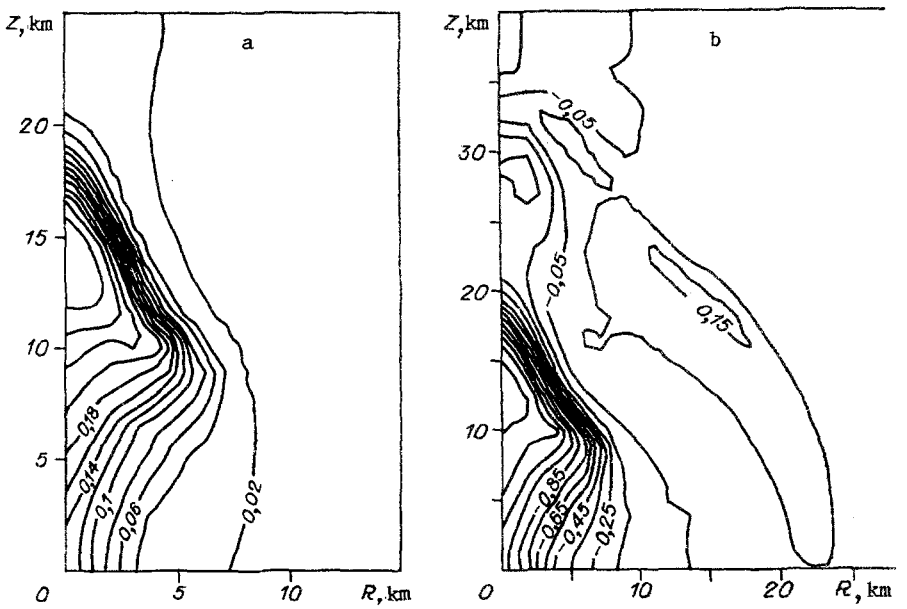

Fig. 11

and tilted at 45° to the surface. Note that the effective temperature $T_{eff} = (I/\sigma)^{1/4}$ is equal to 0.68, 0.60, 0.9, and 0.64 eV at those instants of time. The nonmonotonic change in T_{eff} is a result of gas dynamic processes in the fireball. The radiation spectrum differs widely from that of a blackbody at the indicated instants because the optical thickness along the ray is less than 1.

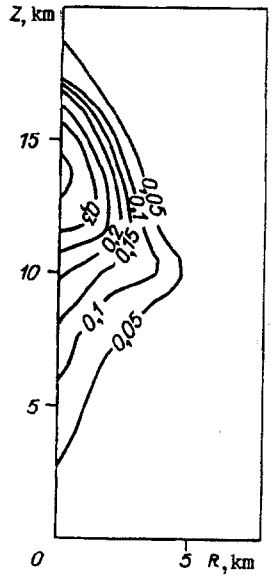

Fig. 12

Most of the emission is in the visible, near ultraviolet, or infrared part of the spectrum. Generally speaking, this emission may be registered by optical apparatus from spaceships, special artificial Mars satellites, or even from the Earth.

Figure 11 shows the distribution of the temperature T (a) and density (b) for t = 60 sec. The location of explosion products (isolines of its concentration) at this point in time is shown in Fig. 12. The center of the explosion products is at a height of 13 km. The cloud is shaped like a jet and not like a ring vortex as it should be for an explosion of the same power near the Earth's surface. This is connected with the fact that at the instant t = 2 sec when the shock wave approaches an altitude equal to the characteristic altitude of Mars' atmosphere, its amplitude is rather high. So, the shock wave passage to the rarefied atmosphere results in gas flow, starting from the surface and following the shock wave. The role of the trace is of great important too, because, for example at the instant t = 2 sec when the shock wave radius is, on the average, 4.5 km, the conic precursor length (2 km) and its radius (1.5 km) are comparable with this value, so the trace promotes the elevation of the hot region and the explosion products. The parameters of the product cloud may also be used in determining the parameter of the impacting body.

For bodies of larger diameter (R $\approx$ 1 km) both the trace radius and the ratio between the diameter of the disturbed region and the characteristic altitude of the atmosphere are large. The explosion generates a powerful jet of velocity greater than the escape velocity (5 km/sec for Mars). It extends the height of the emitting radiation and the surface is rather intense, much as it takes place in impacts on the earth's surface [25]. These impacts may be essential in the evolution of not only Mars' atmosphere, but its surface as well.

Thus, thermal emission is of great importance in all stages of cosmic body impacts on Mars' surface. It results in quantitative changes in the dynamic flow of the nascent gas and in qualitatively new effects. In addition, the radiation emitted by the explosion makes it possible to record experimentally the phenomenon of meteor impact.

REFERENCES

1. H. J. Melosh, "Atmospheric breakup of terrestrial impactors," Proc. Lunar and Planetary Sci. Conf. (eds. P. H. Shultz and R. B. Merril), Pergamon Press, New York (1981), Vol. 12, Part A.
2. I. V. Nemchinov and M. A. Tsikulin, "Estimate of heat transfer with emission for large meteor bodies moving in the Earth's atmosphere with very high velocities," Geomagn. Aèronom., **3**, No. 4 (1962).
3. V. A. Bronshtan, Physics of Meteor Phenomena [in Russian], Nauka, Moscow (1981).
4. V. P. Korobeinikov, P. I. Chushkin, and L. V. Shurshalov, "Simulation and computation of explosion of the Tunguska meteorite," in: Interaction of meteor material with the earth [in Russian], Nauka, Novosibirsk (1980).
5. V. P. Korobeinikov, "Interaction of large bodies with the earth's atmosphere," in: Investigations on Meteorites in Syberia [in Russian], Nauka, Novosibirsk (1984).

6. R. E. McCrosky, Ts. I. Shao, and A. Rosen, "Meteors of Prairie net. General information and orbits," Meteoritika, No. 37, 44-59 (1978).
7. R. E. McCrosky, Ts. I. Shao, and A. Rosen, "Meteors of Prairie net. Trajectories and lustre curves," Meteoritika, No. 38, 106-156 (1977).
8. I. V. Nemchinov, V. V. Novikova, and O. P. Popova, "Analysis of observational results on movement and illuminance of rapid and large meteors in the earth's atmosphere," Meteoritika, No. 48, 124-137 (1989).
9. S. S. Grigoryan, "On meteorite movement and destruction in the atmosphere of planets," Kosm. Issled., **17**, No. 6, 875-893 (1979).
10. T. J. Ahrens and J. D. O'Keefe, "Impact on the Earth, ocean and atmosphere," Int. J. Impact Eng., **5**, 13-32 (1987).
11. H. J. Melosh, Impact Cratering: a Geological Process, Oxford University press and Oxford Claredon Press, New York (1989).
12. Ya. B. Zel'dovich and Yu. Raizer, Physics of Shock Waves and High-Temperature Hydrodynamics Phenomena [in Russian], Nauka, Moscow (1966).
13. L. I. Sedov, Similarity and Dimension Methods in Mechanics [in Russian], Nauka, Moscow (1987).
14. I. V. Nemchinov, V. V. Svettsov, and V. V. Shuvalov, "Solution of the problem of powerful intensely emitting shock wave propagation in air by the method of averaging equations for transfer of emission," in: Low-Temperature Plasma in Space and on the Earth [in Russian], VAGO, Moscow (1977).
15. I. V. Nemchinov, V. V. Svettsov, and V. V. Shulvalov, "Structure of a heated layer ahead of a powerful intensely emitting shock wave front," Zh. Prikl. Mekh. Tekh. Fiz., No. 5 (1978).
16. I. V. Nemchinov, V. V. Svettsov, and V. V. Shuvalov, "Brightness of intense shock waves in air of reduced density," Zh. Prikl. Spektrosk., **30**, No. 6, 1086-1092 (1979).
17. I. V. Nemchinov, I. A. Plozova, V. V. Svettsov, and V. V. Shuvalov, "Computation of one-dimensional explosion with emission," in: Dynamics of Emitting Gas [in Russian], Comp. Center of Acad. of Sci. USSR, Moscow, No. 3, 33-45 (1980).
18. S. A. Losev, N. N. Pilyugin, and S. T. Surzhikov, Simulation of Radiation Processes in Continuum Mechanics, [in Russian], Moscow State Univ., Moscow (1990).
19. S. I. Kas'kova, G. S. Romanov, K. L. Stepanov, and L. K. Stanchits, "Tables of thermophysical characteristics, composition, and radiation losses for multicharged air plasma in local ionizing equilibrium," Zh. Prikl. Spektrosk., **54**, No. 1 (1991), Dep. VINITI N5268-B90.
20. G. S. Romanov, L. K. Stanchits, and K. L. Stepanov, "Tables of average group coefficients of carbon plasma absorption," Dep. Bel. NIINTI, No. 838-BeD84 (1984).
21. A. A. Samarskii and Yu. P. Popov, Difference Schemes in Gas Dynamics [in Russian], Nauka, Moscow (1975).
22. V. I. Moroz, V. V. Kerzhanovich, and V. A. Krasnopol'skii, "Engineer pattern of atmosphere, Mars," Kosm. Issled., **29**, No. 1, 3-84 (1991).
23. J. Ready, Effect of Poweful Laser Emission, Mir, Moscow (1974).
24. V. I. Artem'ev, V. I. Bergel'son, I. V. Nemchinov, et al., "Formation of new structures of gas dynamic flows during density disturbance in thin long channels ahead of shock wave fronts," Mat. Model. **1**, No. 8, 1-11 (1989).
25. I. V. Nemchinov, and V. V. Svettsov, "Radiation gas dynamic processes in the atmosphere during a comet's impact on Earth's surface," Meteoritika, **48**, 141-149 (1989).